



HAL
open science

Mimicking brain tissue binding in an in vitro model of the blood-brain barrier illustrates differences between in vitro and in vivo methods for assessing the rate of brain penetration

Marjolein Heymans, Emmanuel Sevin, Fabien Gosselet, Stefan Lundquist,
Maxime Culot

► To cite this version:

Marjolein Heymans, Emmanuel Sevin, Fabien Gosselet, Stefan Lundquist, Maxime Culot. Mimicking brain tissue binding in an in vitro model of the blood-brain barrier illustrates differences between in vitro and in vivo methods for assessing the rate of brain penetration. *European Journal of Pharmaceutics and Biopharmaceutics*, 2018, 127, pp.453-461. 10.1016/j.ejpb.2018.03.007 . hal-02506299

HAL Id: hal-02506299

<https://univ-artois.hal.science/hal-02506299>

Submitted on 18 Jul 2022

HAL is a multi-disciplinary open access archive for the deposit and dissemination of scientific research documents, whether they are published or not. The documents may come from teaching and research institutions in France or abroad, or from public or private research centers.

L'archive ouverte pluridisciplinaire **HAL**, est destinée au dépôt et à la diffusion de documents scientifiques de niveau recherche, publiés ou non, émanant des établissements d'enseignement et de recherche français ou étrangers, des laboratoires publics ou privés.



Distributed under a Creative Commons Attribution - NonCommercial - NoDerivatives 4.0
International License

1 Mimicking brain tissue binding in an *in vitro* model of the blood-brain barrier illustrates
2 differences between *in vitro* and *in vivo* methods for assessing the rate of brain penetration

3
4 *Authors: HEYMANS¹ Marjolein, SEVIN Emmanuel¹, GOSSELET Fabien¹, LUNDQUIST Stefan² and*
5 *CULOT¹ Maxime*

6
7 ¹Univ. Artois, EA 2465 - Blood-Brain Barrier Laboratory (LBHE), F-62300 Lens, France.

8 ²Local DMPK department, AstraZeneca R&D, Södertälje, Sweden (this facility was
9 discontinued in 2014).

10
11 Corresponding author:

12 Maxime CULOT

13 Address:

14 Univ. Artois, EA 2465 - Blood-Brain Barrier Laboratory (LBHE)

15 Faculté des Sciences Jean Perrin, rue Jean Souvraz, F-62300 Lens, France.

16 Tel: (+33)3 21 79 17 51

17 E-mail: *maxime.culot@univ-artois.fr*

18 **I. Funding Statement**

19 This work was supported by DMPK, AstraZeneca R&D, Södertälje, S-151 85, Sweden and by the
20 European Commission under a Marie Skłodowska-Curie Innovative Training Network: BtRAIN –
21 European Brain Barriers Training Network (H2020-MSCA-ITN-2015, n°675619).

22

23

24

25

26

27

28

29

30

31

32 II. Abstract

33 Assessing the rate of drug delivery to the central nervous system (CNS) *in vitro* has been used
34 for decades to predict whether CNS drug candidates are likely to attain their pharmacological
35 targets, located within the brain parenchyma, at an effective dose. The predictive value of *in*
36 *vitro* blood-brain barrier (BBB) models is therefore frequently assessed by comparing *in vitro*
37 BBB permeability, usually quoted as the endothelial permeability coefficient (P_e) or apparent
38 permeability (P_{app}), to their rate of BBB permeation measured *in vivo*, the latter being
39 commonly assessed in rodents.

40 In collaboration with AstraZeneca (DMPK department, Södertälje, Sweden), the *in vitro* BBB
41 permeability (P_{app} and P_e) of 27 marketed CNS drugs has been determined using a bovine *in*
42 *vitro* BBB model and compared to their *in vivo* permeability (P_{vivo}), obtained by rat *in-situ* brain
43 perfusion. The latter was taken from published data from Summerfield *et al.* (2007).

44 This comparison confirmed previous reports, showing a strong *in vitro/in vivo* correlation for
45 hydrophilic compounds, characterized by low brain tissue binding and a weak correlation for
46 lipophilic compounds, characterized by high brain tissue binding. This observation can be
47 explained by the influence of brain tissue binding on the uptake of drugs into the CNS *in vivo*
48 and the absence of possible brain tissue binding *in vitro*.

49 The use of glial cells (GC) in the *in vitro* BBB model to mimic brain tissue binding and the
50 introduction of a new calculation method for *in vitro* BBB permeability (P_{vitro}) resulted in a
51 strong correlation between the *in vitro* and *in vivo* rate of BBB permeation for the whole set of
52 compounds. These findings might facilitate further *in vitro* to *in vivo* extrapolation for CNS drug
53 candidates.

54

55

56

57

58

59

60

61

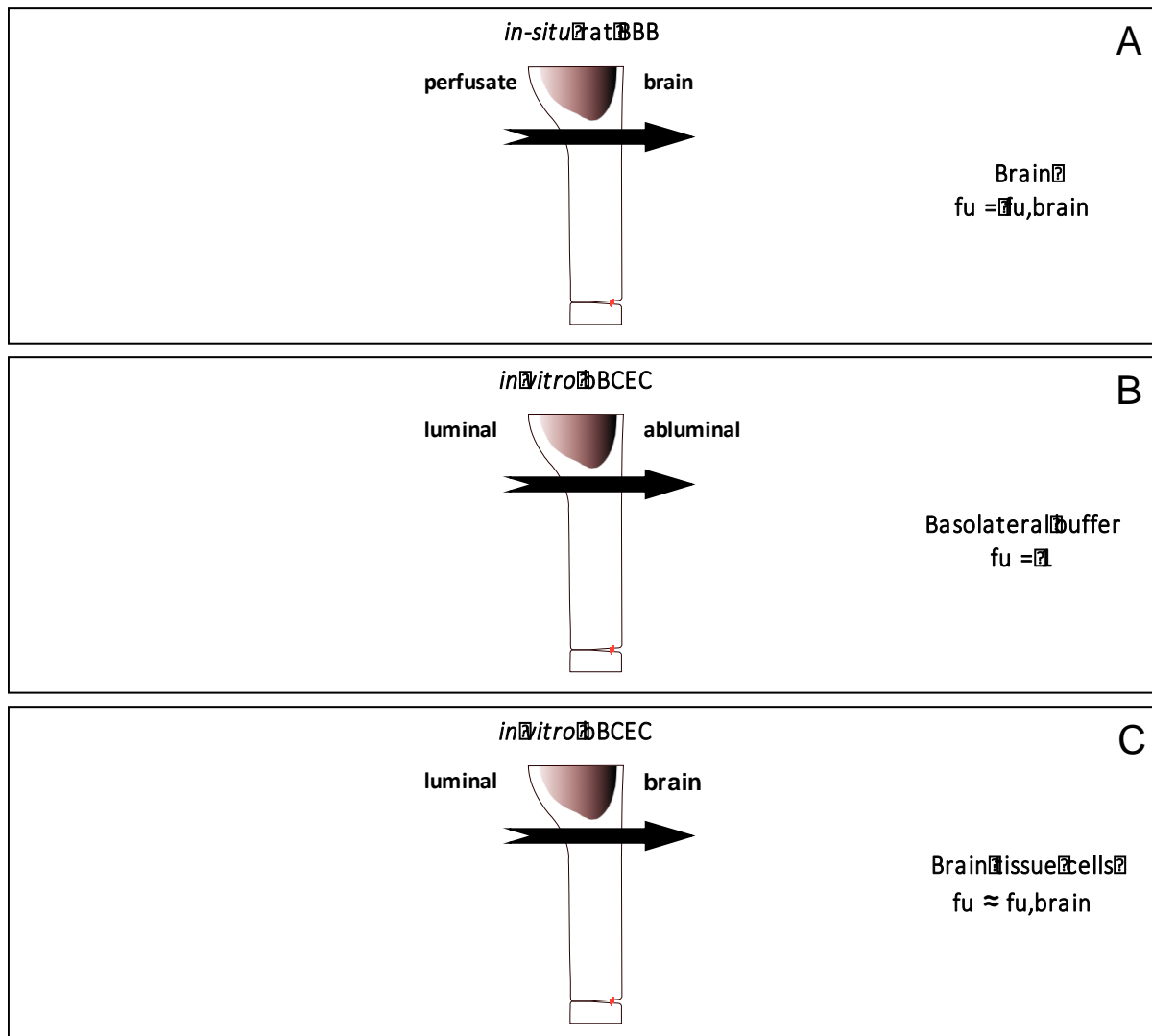
62

63 III. Keywords

64 blood-brain barrier, endothelial cells, brain exposure, drug discovery, BBB permeability, brain
65 tissue binding, *in vitro* model, *in-situ* brain perfusion.

66

67 IV. Graphical Abstract



68

69 V. Abbreviations

70 BBB, blood-brain barrier

71 bBCEC, bovine brain capillary endothelial cells

72 EC, endothelial cells

- 73 CNS, central nervous system
- 74 $f_{u,br}$, fraction unbound brain
- 75 GC, glial cells
- 76 MB, mass balance/compound recovery
- 77 P_{app} , apparent permeability value
- 78 P_e , endothelial permeability coefficient
- 79 PS, permeability surface area product
- 80 PS_e , total PS
- 81 PS_f , filter PS
- 82 PS_t , endothelial PS
- 83 P_{vivo} , *in-situ* brain permeability value
- 84 P_{vitro} , *in vitro* permeability value

85 1. Introduction

86 The development of drugs for treating central nervous system (CNS) disorders is a medically
87 challenging and commercially risky field, which is known to have a high attrition rate [1]. The
88 blood–brain barrier (BBB), which is a major interface between the circulatory system and the
89 brain parenchyma, can hinder a drug candidate’s access to pharmacological targets located
90 within the brain parenchyma. As brain capillaries are the main entry route for the CNS, they
91 can therefore also prevent neuropharmaceuticals from reaching the brain parenchyma at an
92 effective dose. Consequently, the therapeutic potential of a drug candidate is not only related
93 to its activity at the target, but also to its ability to attain an effective dose at the target site.
94 Ideally, this issue should be addressed as early as possible in the drug discovery process [2].
95 Since animal-based assays tend to be time-consuming and require bioanalytical input or access
96 to radiolabelled compounds, they are generally performed at a relatively late stage of
97 development and are not particularly suitable for dealing with the flow of compounds
98 generated by combinatorial chemistry and high-throughput screening. To overcome the
99 limitations of such *in vivo* studies, several animal-free techniques have been developed since
100 the early 90’s for determining the BBB permeability of potential drug candidates [3]. *In vitro*
101 BBB permeability is usually quoted as the endothelial permeability coefficient (P_e) or apparent
102 permeability (P_{app}) and converted to the permeability surface area product that represents the
103 clearance across the BBB into the brain.

104 In many cases, the intended use of *in vitro* BBB permeability in the drug discovery process is to
105 predict whether investigational drugs are likely to achieve a relevant CNS concentration to elicit
106 the desired pharmacological effect. However, BBB permeability is a measurement of the rate
107 of drug delivery to the CNS (i.e. speed at which compounds cross the BBB) which must be
108 considered separately from the extent (e.g. the ratio of drug concentration in the brain and
109 plasma) of equilibration of the drug across the BBB and the intra-brain distribution data in order
110 to fully understand brain drug delivery and its consequences for central drug action [4].

111 Therefore, care should be taken when interpreting results of correlations between *in vitro* and
112 *in vivo* models and when comparing different *in vitro* or *in vivo* approaches as there can be
113 many reasons for divergent results [5]. For instance, in the past, the extent and the rate of
114 transport (i.e. BBB permeability) have sometimes been compared and used indiscriminately [6].
115 Furthermore, since 2002, methods have been developed to estimate drug binding to brain

116 tissue, usually expressed as the fraction unbound brain ($f_{u,br}$, i.e. the ratio of the amount of free
117 drug in the interstitial fluid divided by its total amount in brain tissue). The availability of high-
118 throughput equilibrium dialysis [7,8] or brain slice methods [9] to estimate a drug's $f_{u,br}$ has
119 highlighted that the *in vivo* BBB permeability (i.e. the rate of drug delivery to the CNS) is
120 influenced by their ability to bind to brain tissue [6,10,11]. Consequently, as *in vitro*
121 experimental designs can fail to take into account binding to brain tissue [6,12], this might
122 confound the interpretation of data and generate misleading correlations and conclusions
123 when comparisons between *in vitro* and *in vivo* models are made.

124 The well-tested rodent *in-situ* brain perfusion method [13] enables an accurate assessment of
125 BBB permeability *in vivo* and could therefore be considered as an ideal validation tool for
126 assessing *in vitro* BBB models.

127
128 In collaboration with AstraZeneca (DMPK department, Södertälje, Sweden) the *in vitro*
129 permeability (P_{app} and P_e) of 27 marketed CNS drugs has been determined using a bovine *in*
130 *vitro* BBB model, adapted to high-throughput screening [14], and compared to their *in vivo*
131 permeability (P_{vivo}), obtained by rat *in-situ* brain perfusion. The latter was taken from published
132 data by Summerfield *et al.* (2007) [6]. The selected CNS compounds are covering a wide range
133 of physico-chemical properties and the relationship between their BBB permeability *in vitro*
134 and their binding to brain tissue (based on published $f_{u,br}$) was examined in this study. For this,
135 a new method to assess *in vitro* permeability (P_{vitro}) was used, as it implements brain tissue
136 binding in the assay.

137

138 **2. Material and Methods**

139 *2.1. Test compounds*

140 The marketed CNS compounds were obtained from Sigma-Aldrich (Stockholm, Sweden), except
141 for risperidone, olanzapine, saquinavir, donepezil, venlafaxine and ziprasidone, which were
142 obtained from Sequoia Research Products (Pangbourne, UK). [$U-^{14}C$]-Sucrose was obtained
143 from Perkin-Elmer (Waltham, MA, USA). All other compounds were provided by AstraZeneca
144 R&D, Södertälje, Sweden from in-house sources. Reagents were obtained from Sigma-Aldrich
145 (Stockholm, Sweden).

146

147 All compounds were dissolved at a concentration of 2 μM in Krebs-Ringer HEPES buffer (NaCl
148 150 mM, KCl 5.2 mM, CaCl_2 2.2 mM, MgCl_2 0.2 mM, NaHCO_3 6 mM, Glucose 2.8 mM, HEPES 5
149 mM, water for injection).

150

151 *2.2. Traditional method to assess in vitro BBB permeability (apparent permeability, P_{app} and*
152 *endothelial permeability, P_e)*

153 The traditional method for assessing the *in vitro* BBB permeability is taken from the co-culture
154 model of Dehouck *et al.* (1990) [15], which was slightly modified as described by Culot *et al.*
155 (2008)[14] to adapt it to industrial high throughput screening requirements. In brief, primary
156 bovine brain capillary endothelial cells (bBCECs) were seeded at 6×10^5 cells. mL^{-1} on a semi-
157 permeable membrane (0.4 μm , 24-well system, Millicell-24 cell culture insert plate, Millipore
158 Corporation, MA, USA) coated with rat tail collagen (prepared by using the method of Bornstein
159 (1958) [16], and placed in a single-well feeding cell culture plate (Millipore Corporation, MA,
160 USA). After 3 days, medium was changed to BBB inducing medium (containing 1% of
161 conditioned medium from the traditional glial and EC co-culture) (Cellial Technologies, Lens,
162 France).

163

164 Drug *in vitro* permeability assessment was carried out 1 day later at pH = 7.4 and T = 37°C. At
165 the initiation of the permeability experiments, the receiver wells of a cell-free 24-well plate
166 were filled with 0.8 mL buffered Ringer's solution and filter inserts containing confluent
167 monolayers of bBCEC, were placed in the 24-well plate. The test solution, containing the
168 compound at 2 μM , was added to the bBCEC monolayer at a volume of 0.4 mL and the plate
169 was placed on an orbital shaker (model PX-MIS 6-1, Polymix, Kinematica AG, Switzerland) with
170 low shaking velocity (60 rpm) for exactly 30 minutes. In parallel, the integrity of the bBCEC
171 monolayer was assessed by permeability measurements of either ^{14}C -sucrose (1.813 kBq. mL^{-1})
172 or lucifer yellow (50 μM). Aliquots were taken from the donor solution in the beginning of the
173 experiment (C_0) and from the donor and receiver compartment at the end of the experiment.
174 A total of 3 inserts with and 3 inserts without cells were assessed for each test compound.

175

176 The *in vitro* brain permeability was measured by either the calculation for P_{app} ($\text{cm} \cdot \text{s}^{-1}$) (Equation
177 1) or by the calculation for P_e ($\text{cm} \cdot \text{min}^{-1}$) (Equation 4).

178

179 The P_{app} was calculated as followed:

180

181 Eq. 1:
$$P_{app} = \frac{J}{A.C_0}$$

182

183 With J representing the flux or rate of appearance of the compound in the receiver
184 compartment (amount. s^{-1}); C_0 , the concentration in the donor compartment at t_0 (amount. mL^{-1}); and S, the surface area of the filter insert, which is 0.7 cm^2 for the 24-well format. This results
185 in $cm.s^{-1}$ as the unit for P_{app} .

187 The P_e was calculated as described by Siflinger-Birnboim *et al.* [17]. By dividing the amount of
188 compound in the receiver compartment by the drug concentration in the donor compartment
189 (Eq. 2), the cleared volume (CL in μL) was obtained at each time point.

190

191 Eq. 2:
$$CL = \frac{A_{receiver}}{C_{donor}}$$

192

193 With $A_{receiver}$ representing the amount of the compound in the receiver compartment; and
194 C_{donor} , the concentration of the compound in the donor compartment.

195

196 When the average cumulative CL is plotted over time, the slope equals the permeability surface
197 area product (PS) of the filter. The PS of a filter coated with bBCECs is called the total PS (PS_t)
198 and the PS of a filter without bBCECs is called the filter PS (PS_f). The PS value for the bBCEC
199 monolayer (PS_e) can be computed out of PS_t and PS_f (Equation 3). Units of PS and surface area
200 are $\mu L.min^{-1}$ and cm^2 , respectively.

201

202 Eq. 3:
$$1/PS_e = 1/PS_t - 1/PS_f$$

203

204 To generate P_e ($cm.min^{-1}$), the PS_e value was divided by the surface area of the filter.

205

206 Eq. 4:
$$P_e = \frac{PS_e}{S}$$

207

208 To assess possible adsorption to plastic or non-specific binding to cells, the mass balance (MB,
209 %) was calculated from the amount of recovered compound in both compartments at the end

210 of the experiment divided by the total amount of compound added in the donor compartment
211 at t_0 .

212

213 2.3. New method to assess *in vitro* BBB permeability (P_{vitro})

214 The new *in vitro* permeability (P_{vitro}) was obtained by using the same protocol as the traditional
215 method explained above, but with some modifications in experimental design and calculation
216 method.

217 Primary cultures of mixed glial cells (GC) were prepared from the cerebral cortex of new-born
218 rats. After removing the meninges, the brain tissue was forced gently through a nylon sieve.
219 Glial cells were plated on 6-well dishes (Nunc, Roskilde, Denmark) at a concentration of $1.2 \times$
220 10^5 cells.mL⁻¹ in 2 mL DMEM supplemented with 10% (v/v) fetal calf serum (Hyclone
221 Laboratories). The medium was changed twice a week. Three weeks after seeding, cultures of
222 GC were stabilized and composed of astrocytes (60%, characterized with glial fibrillary acidic
223 protein), oligodendrocytes (30%, characterized with O4) and microglial cells (10%,
224 characterized with ED-1).

225 As explained above, 1×10^6 cells of bBCECs were seeded on a gelatin-coated Petridish (100 mm
226 diameter, Corning). After 2 days, the bBCECs are subcultured in Transwell inserts (0.4 μ m pore
227 size, 6-well system, Corning Incorporate) coated with rat tail collagen and placed in a, with
228 stabilized primary rat GC seeded, 6-well. After 12 days in the incubator at 37°C and 5 % CO₂,
229 drug *in vitro* permeability assessments were carried out at pH = 7.4 and T = 37°C.

230

231 At the initiation of the permeability experiment, the receiver wells of a 6-well plate containing
232 the primary rat GC, were rinsed twice with 5 mL and filled with 2.5 mL buffered Ringer's solution
233 and Transwell inserts containing confluent monolayers of bBCECs, were placed in the 6-well
234 plate. The test solution, containing the compound at 2 μ M, was added to the bBCEC monolayer
235 at a volume of 1.5 mL and the plate was placed on an orbital shaker (model PX-MIS 6-1, Polymix,
236 Kinematica AG, Switzerland) with low shaking velocity (60 rpm) for exactly 60 minutes. In
237 parallel, the integrity of the bBCEC monolayer was assessed by permeability measurements of
238 either ¹⁴C-sucrose (1.813 kBq.mL) or lucifer yellow (50 μ M). Aliquots were taken from the donor
239 solution in the beginning of the experiment (C_0) and from the donor and receiver compartment
240 at the end of the experiment. A total of 3 inserts with and 3 inserts without cells were assessed
241 for each test compound.

242 All samples were analysed using tandem mass spectrometry (cfr. *Analytical procedures*) and
243 raw data were computed using the blue-norna[®] calculator to generate P_{vitro} (cm.min⁻¹)
244 according to the following equations (Equation 5 and 6):

245

246 Eq. 5:
$$in\ vitro\ K_{in,t} = \frac{(C_{donor,0} - C_{donor,end}) \times V_{donor}}{C_{donor,end} \times T}$$

247

248 Eq. 6:
$$P_{vitro} = \frac{in\ vitro\ K_{in}}{S}$$

249

250 Where C_{donor} (in mM) is the concentration of compound in the donor compartment at either
251 the onset or end of the transport experiment, T (in min) is the duration of the permeability
252 experiment, V_{donor} (in mL) is the volume of the donor compartment, which is 1.5 mL and S is
253 the surface area of the Transwell insert (i.e. 4.67 cm²).

254

255 2.3. *Analytical procedures*

256 The amount of the radiolabel (¹⁴C-sucrose) and fluorescent label (lucifer yellow) were
257 determined by liquid scintillation (Packard Instrument Company, Meriden, USA) and
258 fluorescence spectrophotometry (Synergy H1, BioTek Instruments SAS, Colmar, France),
259 respectively. For the measurement of lucifer yellow, an excitation wavelength of 432 and an
260 emission wavelength of 538 was used. A blank value was subtracted from the measured values.

261

262 All CNS compounds were determined by the liquid chromatography – mass spectrometry
263 (LC/MS) method. All samples were analysed using the following instruments: mass
264 spectrometer, Quattro Premier XE (Waters); autosampler, acquity sample manager; UPLC
265 pump, acquity binary solvent manager (Waters); robot for sample preparation, Biomek FX
266 (Beckman- Coulter). The following chemicals and reagents were used: ammonium acetate
267 (Merck), acetonitrile gradient grade (Merck), methanol gradient grade (Merck), laboratory
268 deionised water, further purified with a Milli-Q water purifying system and ammonium acetate
269 1 mol/L in milli-Q water. Samples were stored in -20°C. Prior to analysis, samples were thawed
270 and shaken. If reanalysis was necessary, samples were stored overnight at 10 °C (in an auto
271 sampler).

272 For chromatography, the following system was used: analytical column, acquity UPLC BEH C18
273 1.7 μm , 2.1 x 30 mm (Waters). Eluent A was 10 mM ammonium acetate containing 2%
274 acetonitrile and Eluent B was 10 mM ammonium acetate containing 80% acetonitrile. The flow
275 rate was 0.6 mL.min⁻¹ (loop: 10 μL , injection volume: 5-10 μL). The gradient started at 0.2 min
276 with 2% of Eluent B and increased to 100% of Eluent B within 0.3 min followed by a column
277 washing step at 100% of Eluent B for 0.2 min.

278 Quantification of unknown samples was performed, using QuanLynx software. Response
279 factors were constructed by plotting peak area of the analyte against concentration of each
280 analyte using an average response factor of the donor (D_0/C_0) sample injections. The average
281 RF function without weighting was used.

282

283 **3. Results and Discussion**

284 In this study, the *in vitro* BBB transport of 27 CNS compounds has been assessed and the
285 relationship between either their P_{app} or P_e values *in vitro* and their *in vivo* permeability was
286 compared. To evaluate the influence of brain tissue binding in BBB transport, the compounds
287 were arbitrarily classified in four categories of $f_{u,\text{br}}$ (Table 1). Both *in vivo* permeability and $f_{u,\text{br}}$
288 data were obtained from one single study of Summerfield *et al.* (2007) [6] (Table 2).

289

290 Several authors tend to use the P_{app} calculation when assessing BBB permeability, while other
291 used the P_e calculation which also accounts for the ability of the compound to cross the cell
292 culture insert. The latter therefore required the assessment of the permeability of the
293 compounds over inserts without cells (PSf).

294 Although the ability of the compounds to cross the filter is not accounted for in the P_{vitro}
295 calculation, the distribution of the compounds across similar collagen coated inserts (i.e. 6 well-
296 system) without cells has been assessed. All compounds were considered to not be limited by
297 their ability to cross the coated insert. This was based on the sufficient amount of compounds
298 found in the receiver compartment at the end of the one hour transport experiment (i.e. more
299 than 20% of initial amount – data not shown).

300

301

302

303 **Table 1** – *In vitro* BBB permeability values for the 27 CNS drugs under study obtained by the traditional
 304 method (P_{app} and P_e). The permeability values are accompanied by their corresponding (average) mass
 305 balance value (MB). The MB was also measured in absence of bovine brain capillary endothelial cells
 306 (bBCEC or EC).

	Compound name	P_{app} (+ EC, - GC)		P_e (+ EC, - GC)		Average MB	
		$(10^{-6} \text{ cm.s}^{-1})$		$(10^{-3} \text{ cm.min}^{-1})$		- EC, - GC	+ EC, - GC
		Mean	S.D.	Mean	S.D.	%	%
$fu > 0.1$	Bupropion	5.55	1.12	20.81	1.60	n.d.	87
	Carbamazepine	5.15	1.51	11.42	0.80	105	100
	Donepezil	5.43	2.28	18.01	1.70	86	77
	Gabapentin	0.93	0.09	0.79	0.10	112	103
	Sumatriptan	0.87	0.01	0.76	0.10	n.d.	89
	Venlafaxine	4.91	2.53	11.30	1.50	106	99
$0.1 > fu > 0.05$	Mirtazapine	5.09	3.16	25.12	2.10	n.d.	71
	Phenytoin	4.16	0.72	7.71	0.40	101	92
	Risperidone	3.91	1.28	11.12	1.00	90	83
	Selegiline	4.97	2.53	13.30	0.70	82	83
	Trazodone	4.60	0.49	23.15	2.50	n.d.	82
$0.05 > fu > 0.01$	Atomoxetine	3.17	2.59	5.43	0.70	n.d.	63
	Citalopram	4.10	0.81	5.99	1.10	108	87
	Diazepam	5.20	2.52	18.56	1.80	99	90
	Doxepin	4.73	2.54	7.89	0.30	104	77
	Loxapine	3.75	1.93	9.40	1.30	n.d.	60
	Mesoridazine	2.97	0.92	6.57	0.90	n.d.	59
	Olanzapine	5.38	1.06	16.01	1.60	111	97
$0.01 > fu$	Amitriptyline	3.14	2.28	5.49	0.20	73	66
	Chlorpromazine	2.01	2.62	2.51	0.30	51	34
	Fluoxetine	3.79	1.98	8.42	1.20	83	66
	Maprotiline	2.20	2.06	3.85	0.80	n.d.	44
	Perphenazine	0.95	1.32	0.98	0.10	49	33
	Sertraline	1.11	3.23	1.10	0.40	51	26
	Thiothixene	0.72	1.29	0.91	0.10	n.d.	34
	Thioridazine	1.03	1.33	1.30	0.10	41	23
	Ziprasidone	1.50	0.71	2.56	0.30	84	50

307
 308 As exposure to CNS drugs might affect the tightness of the *in vitro* BBB during the BBB
 309 permeability assessment of the drug, the integrity of the bBCEC monolayer during the drug
 310 permeability experiment was assessed in parallel by the permeability assessment of either the
 311 radiolabel ^{14}C -sucrose or the fluorescent label lucifer yellow. All BBB permeability results
 312 presented here correspond to experiments where P_e for the marker molecule(s), in presence
 313 of the tested compounds, did not result in a significant increase compared to a control
 314 experiment without the tested compounds.

315
 316
 317

318 **Table 2** – Physico-chemical characteristics: fraction unbound brain ($f_{u,br}$) and lipophilicity (LogP) and the
 319 *in vivo* blood-brain barrier (BBB) permeability (P_{vivo}) for the 27 CNS drugs under study determined by
 320 Summerfield et al. (2007) [6].

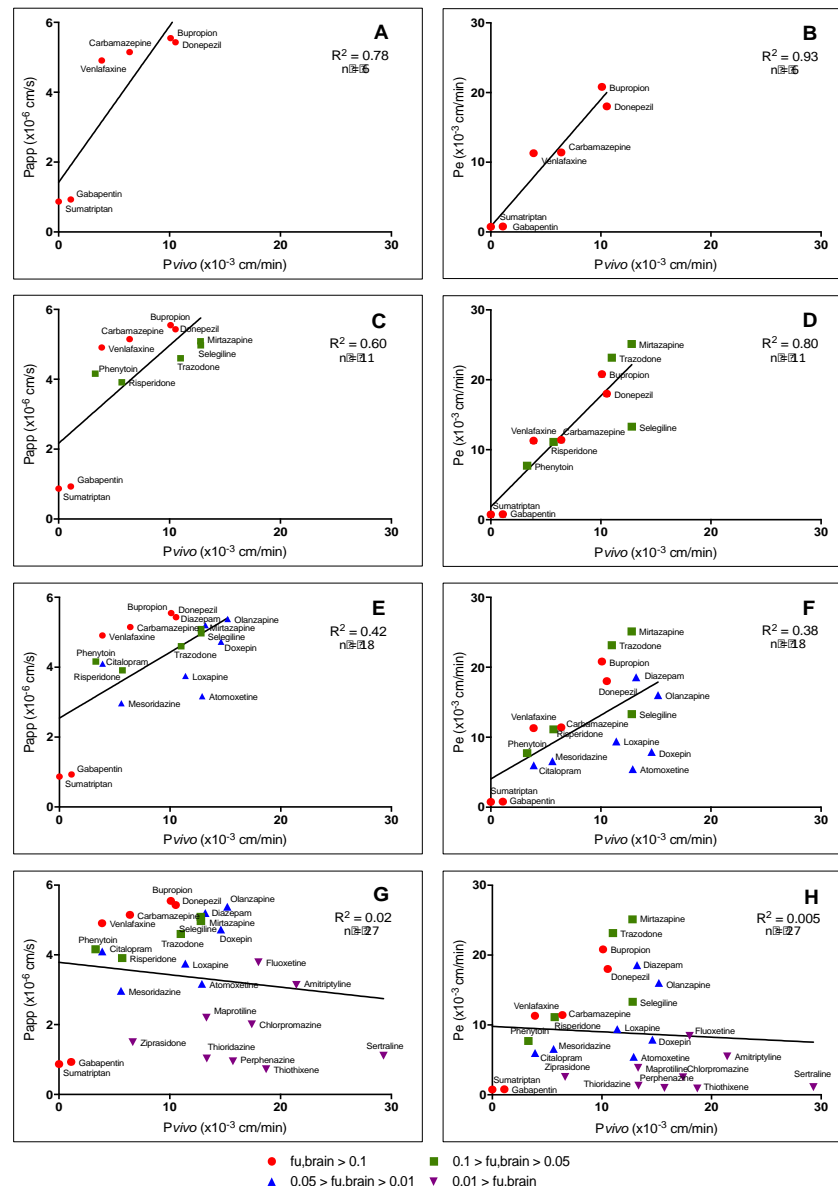
	Compound name	$f_{u,br}$		LogP	P_{vivo} ($10^{-3} \text{ cm}\cdot\text{min}^{-1}$)	
		Mean	S.D.		Mean	S.D.
$f_u > 0.1$	Bupropion	0.171	0.0270	3.27	10.10	1.00
	Carbamazepine	0.119	0.0070	2.10	6.40	1.40
	Donepezil	0.126	0.0150	4.14	10.54	2.53
	Gabapentin	0.782	0.1490	-1.90	1.10	0.07
	Sumatriptan	0.724	0.0690	1.17	0.01	0.01
	Venlafaxine	0.216	0.0230	2.69	3.89	2.90
$0.1 > f_u > 0.05$	Mirtazapine	0.080	0.0030	2.90	12.80	5.00
	Phenytoin	0.082	0.0060	2.26	3.30	0.60
	Risperidone	0.099	0.0030	3.27	5.70	1.27
	Selegiline	0.074	0.0030	3.08	12.81	3.00
	Trazodone	0.055	0.0060	2.68	11.00	0.40
$0.05 > f_u > 0.01$	Atomoxetine	0.019	0.0060	3.95	12.90	3.60
	Citalopram	0.049	0.0040	3.58	3.90	0.67
	Diazepam	0.036	0.0050	2.63	13.20	3.07
	Doxepin	0.025	0.0030	4.08	14.61	2.70
	Loxapine	0.011	0.0030	3.18	11.40	2.27
	Mesoridazine	0.016	0.0010	3.83	5.60	0.87
	Olanzapine	0.034	0.0090	3.61	15.20	0.93
$0.01 > f_u$	Amitriptyline	0.009	0.0010	5.10	21.43	2.93
	Chlorpromazine	0.002	0.0004	5.18	17.40	4.10
	Fluoxetine	0.004	0.0010	4.09	18.00	2.27
	Maprotiline	0.006	0.0027	4.89	13.30	3.30
	Perphenazine	0.004	0.0002	4.15	15.70	1.60
	Sertraline	0.001	0.0001	5.06	29.30	8.27
	Thiothixene	0.003	0.0004	4.01	18.70	3.47
	Thioridazine	0.001	0.0040	5.93	13.34	2.07
	Ziprasidone	0.001	0.0001	4.64	6.65	0.73

321
 322 3.1. Relationship between P_{app} and P_e with P_{vivo} for compounds with decreasing $f_{u,br}$
 323 We evaluated the relationship between BBB permeability *in vitro* (i.e. P_e and P_{app}) and *in vivo*
 324 (i.e. P_{vivo}) for compounds with decreasing $f_{u,br}$. The latter data (i.e. P_{vivo}) was coming from
 325 literature [6].
 326 Strong correlations between P_{vivo} and, either *in vitro* P_{app} (Figure 1A) or P_e (Figure 1B), are
 327 obtained for compounds characterized by an $f_{u,br} > 0.1$ ($n = 6$, $R^2 = 0.78$, $p = 0.0204$ for P_{app} ; and
 328 $n = 6$, $R^2 = 0.93$, $p = 0.0017$ for P_e) and $f_{u,br} > 0.05$ (Figure 1C and D, $n = 11$, $R^2 = 0.60$, $p = 0.0052$
 329 for P_{app} ; and $n = 11$, $R^2 = 0.80$, $p = 0.0002$ for P_e).
 330 The stronger correlation between P_{vivo} and P_e than between P_{vivo} and P_{app} confirms previous
 331 works and supports the use of the P_e calculation in such study [14,18]. The good correlation
 332 between *in vitro* and *in vivo* permeability confirms previous findings showing that this *in vitro*

333 BBB model is highly predictive for the *in vivo* rate of brain penetration for several CNS
 334 compounds [14].

335 However, the same correlation appears very weak after the inclusion of compounds into the
 336 dataset characterized by an $f_{u,br}$ between 0.05 and 0.01 (Figure 1E and 1F, $n = 18$, $R^2 = 0.42$, p
 337 $= 0.0036$ for P_{app} ; and $n = 18$, $R^2 = 0.38$, $p = 0.066$ for P_e). No correlation is shown after the
 338 inclusion of compounds with an $f_{u,br} < 0.01$ (Figure 4G and 4H, $n = 27$, $R^2 = 0.02$, $p = 0.4900$ for
 339 P_{app} ; and $n = 27$, $R^2 = 0.005$, $p = 0.7296$ for P_e).

340



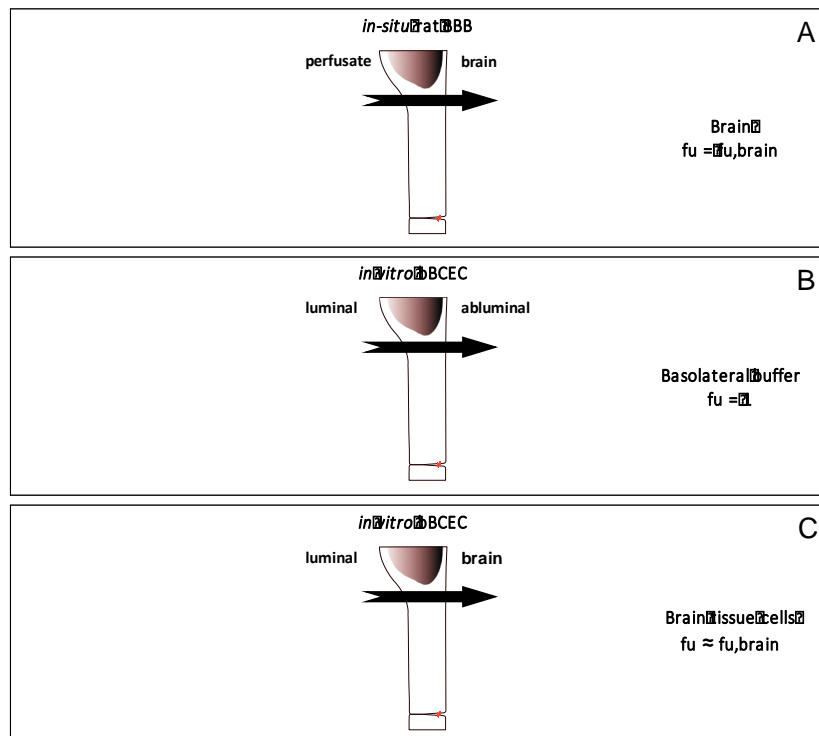
341

342 **Figure 1** – Relationship between *in vivo* brain permeability (P_{vivo}), obtained by brain perfusion in rodents,
 343 taken from Summerfield et al. (2007) [6], and *in vitro* BBB permeability, either depicted by the apparent
 344 permeability (P_{app}) (Graph A, C, E and G), or by the endothelial permeability (P_e) (Graph B, D, F and H),
 345 and this for compounds of decreasing $f_{u,br}$.

346 3.2. Relationship between P_{vivo}/P_{app} and P_{vivo}/P_e and $f_{u,br}$

347 The observed discrepancies between P_{vivo} and *in vitro* P_e or P_{app} for compounds with low $f_{u,br}$
348 corroborates what has been published by several other investigators i.e. that *in vivo*
349 permeability is a composite function of both permeability across the BBB and brain tissue
350 binding, whereas *in vitro* permeability uncouples non-specific binding (Figure 2) [6]. An
351 important note here is that the perfusate used to determine the *in vivo* permeability is Krebs-
352 Ringer HEPES buffer, and therefore, P_{vivo} does not account for plasma protein binding.

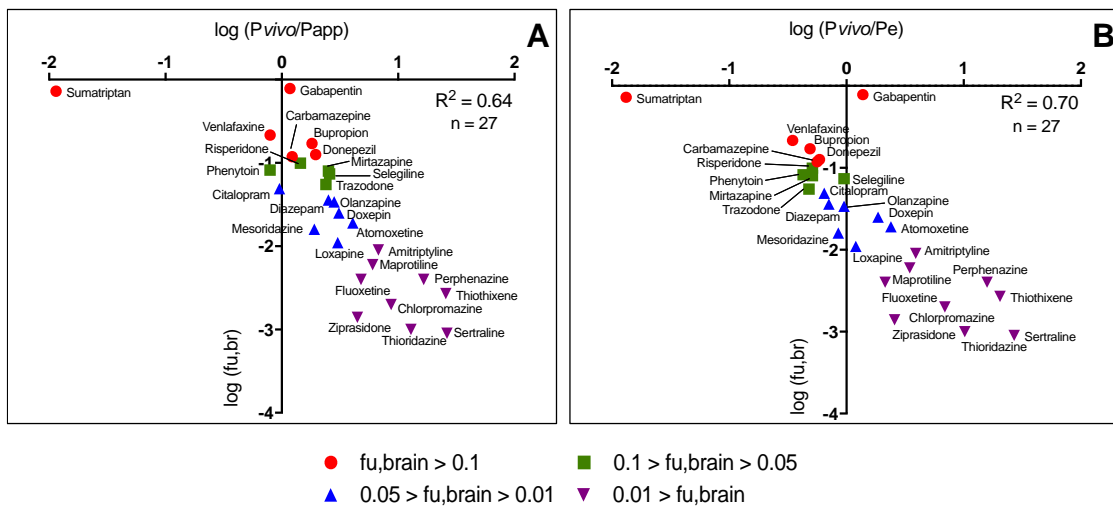
353



354
355 **Figure 2** – Differences in $f_{u,br}$ depending on the experimental design of the model: A) *In-situ* rat BBB model,
356 B) *In vitro* bovine BBB model (consisting of bBCEC) without glial cells (GC) in the receiver compartment
357 during the drug permeability experiment; and C) *In vitro* BBB model (consisting of bBCEC) with GC in the
358 receiver compartment during the drug permeability experiment.

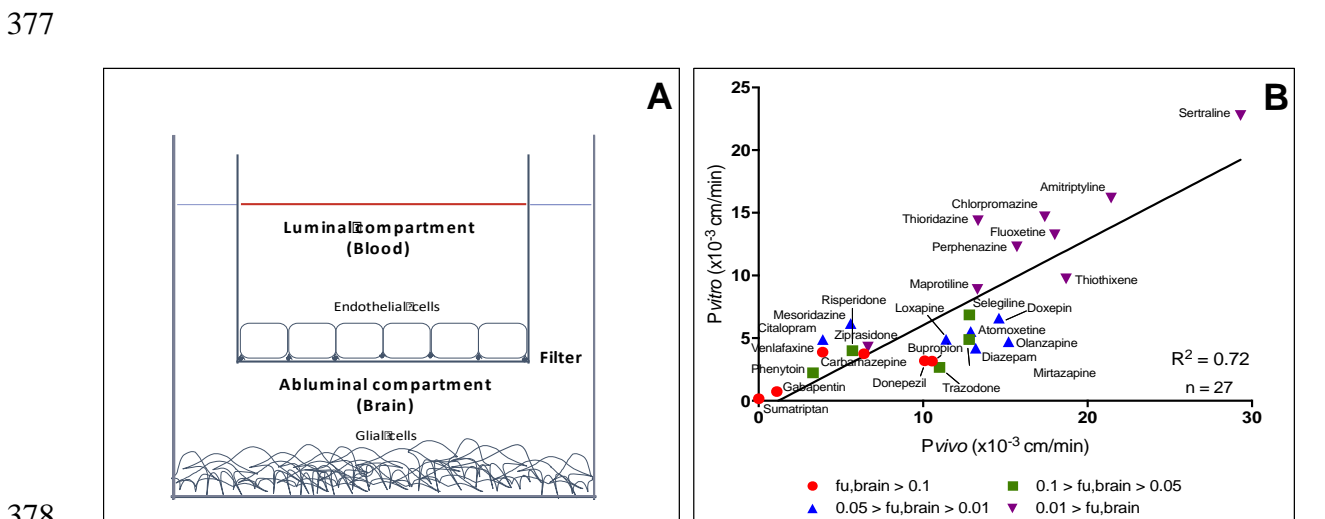
359

360 Indeed, it can be observed that the lack of correlation is mainly due to several lipophilic
361 compounds characterized by high tissue binding. This indicates that brain tissue binding may
362 confound actual *in vivo* permeability *in-situ* and that the observed low *in vitro* permeability for
363 these compounds may be a true reflection of their diffusion process across the BBB. This is
364 supported by the relationship between $f_{u,br}$ and P_{vivo}/P_{app} (Figure 3A, $n = 27$, $R^2 = 0.64$, $p <$
365 0.0001) or by the relationship between $f_{u,br}$ and P_{vivo}/P_e (Figure 3B, $n = 27$, $R^2 = 0.70$, $p < 0.0001$).



366
 367 **Figure 3** – Relationship between $f_{u,br}$ and A) P_{vivo}/P_{app} ; and B) P_{vivo}/P_e . Regression analysis included all
 368 compounds ($n = 27$). P_{vivo} values used for the different ratios were taken from Summerfield et al. (2007)
 369 [6].
 370

371 Based on previous findings i.e. that discrepancies between P_{vivo} and *in vitro* permeability is
 372 related to brain tissue binding, we have developed a new *in vitro* method to obtain the *in vitro*
 373 permeability which accounts for brain tissue binding, P_{vitro} . This new *in vitro* method, and the
 374 corresponding parameter, therefore improves the predictive power of the *in vitro* assay. This
 375 new method is based on the presence of glial cells (GC) in the receiver compartment to mimic
 376 the effect of brain tissue binding *in vivo* during the permeability experiment (Figure 4A).



378
 379 **Figure 4** – A) General scheme of the *in vitro* BBB model from Dehouck et al. (1990) [15]. Bovine brain
 380 capillary endothelial cells (bBCEC) are cultured on the upper side of a permeable support and primary rat
 381 glial cells (astrocytes, oligodendrocytes and microglia) are cultured at the bottom of the well. B)
 382 Relationship between *in vivo* brain permeability (P_{vivo}), taken from Summerfield et al. (2007) [6], obtained
 383 by brain perfusion in rodents, and *in vitro* BBB permeability, obtained by the new *in vitro* method (P_{vitro})
 384 for all 27 compounds under study.

385 3.3. Relationship between P_{vivo} and P_{vitro}

386 In comparison to P_{app} and P_e , the correlation between P_{vitro} and P_{vivo} for all 27 compounds is
 387 significantly improved (Figure 4B, $n = 27$, $R^2 = 0.72$, $p < 0.0001$). This highlights the interest of
 388 the introduced new method as no correlation was found between P_{vivo} and *in vitro* P_{app} or P_e for
 389 the same dataset, consisting of compounds with different physico-chemical properties and $f_{u,br}$
 390 (Table 3) (Figure 1G and 1H).

391

392 **Table 3** – *In vitro* BBB permeability values obtained for the 27 CNS drugs under study by the new method
 393 to assess BBB permeability (P_{vitro}). Permeability values are given for measurements in presence of glial
 394 cells and consist of a corresponding (average) mass balance value (MB).

<i>fu</i> group	Compound name	P_{vitro} (+ EC, + GC)		Average MB
		$(10^{-3} \text{ cm} \cdot \text{min}^{-1})$		(+ EC, + GC)
		Mean	S.D.	%
<i>fu</i> > 0.1	Bupropion	3.19	0.53	87
	Carbamazepine	3.75	1.06	86
	Donepezil	3.16	0.53	79
	Gabapentin	0.74	0.53	98
	Sumatriptan	0.17	0.02	131
	Venlafaxine	3.88	1.06	83
0.1 > <i>fu</i> > 0.05	Mirtazapine	4.89	1.60	69
	Phenytoin	2.24	0.53	99
	Risperidone	4.00	1.06	73
	Selegiline	6.86	2.13	81
	Trazodone	2.66	0.53	92
0.05 > <i>fu</i> > 0.01	Atomoxetine	5.53	2.13	61
	Citalopram	4.89	1.06	64
	Diazepam	4.20	0.53	77
	Doxepin	6.60	1.06	58
	Loxapine	4.90	1.60	60
	Mesoridazine	6.17	1.60	62
	Olanzapine	4.72	0.53	68
0.01 > <i>fu</i>	Amitriptyline	16.17	3.72	33
	Chlorpromazine	14.68	3.19	28
	Fluoxetine	13.24	2.13	34
	Maprotiline	8.88	1.60	41
	Perphenazine	12.29	1.60	34
	Sertraline	22.77	2.66	19
	Thiothixene	9.73	2.13	38
	Thioridazine	14.36	1.06	44
	Ziprasidone	4.28	1.06	44

395

396 The new calculation method is based on the compound's clearance from the donor
 397 compartment with the assumption that the cleared compound is entering the brain.

398 To further evaluate the impact of GC in the *in vitro* BBB model during the permeability
 399 experiment, and to rule out that the observed difference between P_{vitro} and P_e was solely

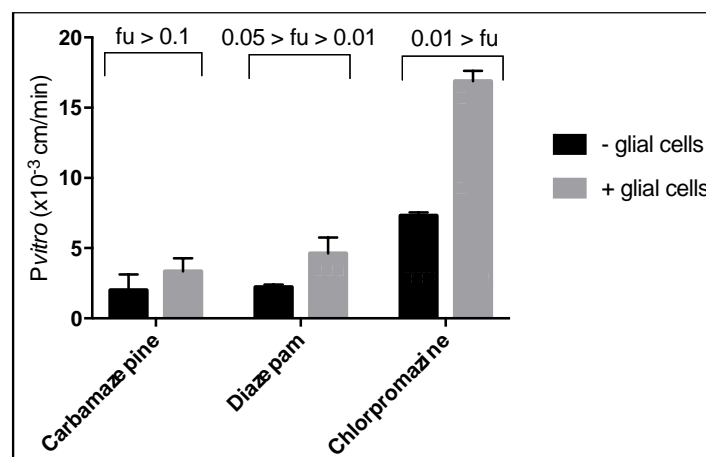
400 attributed to the different calculation method, P_{vitro} was calculated in presence and absence of
 401 GC for 3 different compounds (i.e. carbamazepine, diazepam and chlorpromazine)
 402 characterized by different $f_{u,br}$ (Table 4) (Figure 5).

403

404 **Table 4** – *In vitro* BBB permeability values obtained for 3 CNS drugs (i.e. carbamazepine, diazepam and
 405 chlorpromazine) by the new method to assess BBB permeability *in vitro* (P_{vitro}). The P_{vitro} values are given
 406 for measurements in presence and absence of glial cells (GC) and consist of a corresponding (average)
 407 mass balance value (MB). The MB for the condition without bBCEC (or EC) is also given.

f_u group	Compound name	Average	P_{vitro}		MB	P_{vitro}		Average
		MB	$(10^{-3} \text{ cm.min}^{-1})$			$(10^{-3} \text{ cm.min}^{-1})$		MB
		(- EC, - GC)	(+ EC, - GC)	(+ EC, - GC)	(+ EC, + GC)	(+ EC, + GC)		
		%	Mean	S.D.	%	Mean	S.D.	%
$f_u > 0.1$	Carbamazepine	92	2.01	1.11	89	3.75	1.06	86
$0.05 > f_u > 0.01$	Diazepam	100	2.22	0.18	89	4.20	0.53	91
$0.01 > f_u$	Chlorpromazine	95	7.30	0.24	53.3	14.68	3.19	32

408



409

410 **Figure 5** – Comparison of P_{vitro} in presence and absence of glial cells for 3 compounds (i.e. carbamazepine,
 411 diazepam and chlorpromazine) characterized by a different $f_{u,br}$.

412

413 As expected, the presence of GC during the *in vitro* permeability experiment did not resulted
 414 in a significant difference between P_{vitro} (with and without GC) for compounds with a relatively
 415 high $f_{u,br}$, such as carbamazepine. In contrast, the P_{vitro} of diazepam and chlorpromazine, two
 416 compounds with a relatively low $f_{u,br}$, is higher in presence of GC during the BBB permeability
 417 experiment than in their absence (Figure 5). This result illustrates that a difference between P_e
 418 or P_{app} and P_{vitro} is not an effect of the use of a different calculation method of BBB permeability,
 419 but rather reflects the effect of brain tissue binding on the distribution of the compound in the
 420 *in vitro* assay.

421 Indeed, the difference in brain tissue binding affinity for carbamazepine, diazepam, and
422 chlorpromazine, indicated by their $f_{u,br}$, is also reflected *in vitro* by the mass balance (MB). In
423 presence of GC, the MB is much lower for chlorpromazine than for diazepam and
424 carbamazepine (Table 4). This poor recovery of chlorpromazine in the presence of GC (and to
425 a lower extent of diazepam) reflects the sequestration of the compound within the bBCEC and
426 GC, as the MB of the three compounds in the conditions without either bBCEC or GC does not
427 suggest a strong binding to plastic.

428
429 Altogether, our results support that permeability *in vivo* is a composite function of both
430 permeability across the BBB and tissue binding [4,6]. This can be illustrated by compounds such
431 as chlorpromazine, which has a high permeability *in vivo* (i.e. $P_{vivo} = 17.40 \times 10^{-3} \text{ cm.min}^{-1}$) but
432 one of the lowest permeability *in vitro* (i.e. $P_e = 2.51 \times 10^{-3} \text{ cm.min}^{-1}$). The reason for this
433 discrepancy is not necessarily that the *in vitro* prediction based on the calculation of P_e is wrong,
434 but simply that when chlorpromazine is assessed *in vivo*, a large portion may be associated with
435 the endothelial cell wall. Therefore, when the whole brain is subsequently homogenized, some
436 of the compound associated with the endothelial cell wall, will be erroneously interpreted as
437 having permeated the BBB. In this *in vivo* dataset, the total brain concentration of a compound
438 was corrected based on the apparent brain distribution volume of atenolol to compensate for
439 drug contained in the capillary vascular space [6]. Atenolol is a drug that does not significantly
440 accumulate in brain tissue during the time course of the experiment.

441 In fact, *in vitro* MB calculations indicate that a large portion of chlorpromazine is associated
442 with the bBCEC, as shown by the low recovery in presence of bBCEC and this even in absence
443 of GC. In complete absence of cells (i.e. bBCEC and GC), the recovery of chlorpromazine in this
444 format was close to 100 % and demonstrated the absence of non-specific binding to plastic.
445 Consequently, it may very well be the case that chlorpromazine is slowly diffusing across the
446 BBB, as the *in vitro* permeability data suggests.

447 By combining *in vitro* permeation across the brain endothelium and binding to brain tissue, this
448 new method (i.e. P_{vitro}) offers an improved correlation with *in vivo* data, that we obtained from
449 literature [6]. Although this can be seen as an advantage, it should be noted that the use of the
450 traditional *in vitro* BBB permeability assay could still be valuable as it assesses the BBB
451 permeability without accounting for non-specific binding to brain tissue. This is important

452 information to consider while trying to integrate pharmacokinetic parameters into a coherent
453 model of brain penetration and distribution.

454

455 **4. Conclusion**

456 This study provides a better understanding of the use of *in vitro* BBB models as a tool to predict
457 brain exposure *in vivo*. In this study, 27 CNS compounds were assessed for their BBB
458 permeability *in vitro*, the latter being compared with *in vivo* permeability values obtained from
459 literature [6]. A lack of correlation for highly lipophilic compounds (and a very low $f_{u,br}$) is
460 observed when using the traditional method to assess BBB permeability *in vitro*, which suggests
461 a rather poor predictive power of the traditional permeability assay. As a remark it should be
462 stated that this bovine BBB model has been used both at University of Artois and in house at
463 AstraZeneca (former local DMPK group, Södertälje, Sweden) for more than a decade to predict
464 BBB permeability of compounds [19]. For this, it is likely that numerous compounds having the
465 same characteristics as chropromazine (i.e. highly lipophilic, very low MB) have been screened
466 in this assay. However, as a rule of control, bBCEC integrity and MB were and are always
467 assessed prior the use of the obtained experimental data in permeability calculations. No
468 permeability calculation was performed when the MB was having a value lower than 80 %, as
469 a poor MB could be an indication of several factors e.g. intracellular accumulation of the
470 compound, metabolization of the compound within the endothelium or a lack of accuracy of
471 the used quantification method. Consequently, the resulting poor predictive value obtained by
472 the *in vitro* BBB model compared to the *in vivo* permeability could not be identified.

473 It is only by categorizing compounds based on their $f_{u,br}$ that the observed discrepancy could
474 be identified. This shows and confirms what was already published by several authors, that
475 brain tissue binding is influencing the rate of brain penetration for highly lipophilic compound
476 [6,10,11]. This suggests that the lack of correlation between *in vitro* and *in vivo* permeability
477 values is not necessarily due to a poor *in vitro* permeability assay, but rather to the difference
478 in experimental design. The traditional *in vitro* permeability assay lacks brain tissue and so,
479 provides no possibility for compounds to bind to brain tissue. The contrary is true in case of the
480 *in-situ* brain perfusion method, where compounds face the brain parenchyma after passing the
481 BBB.

482

483 By making use of GC to mimic brain tissue binding *in vitro*, the method that is introduced here
484 provides *in vitro* BBB permeability values that better correlate with *in vivo* permeability values.
485 These results highlight the influence of brain tissue binding, which is sometimes neglected in
486 similar studies and might therefore facilitate *in vitro* to *in vivo* extrapolation, as well as the
487 integration of *in vitro* data into physiologically based pharmacokinetic models of CNS drug
488 distribution.

489
490 The recent development of *in vitro* BBB models in which bBCEC are cultivated in close proximity
491 with other brain cells such as brain pericytes [20] or neuronal progenitors [21] might also
492 benefit of the introduction of the P_{vitro} calculation method, as the same cells (e.g. brain
493 pericytes, neuronal progenitors, etc.) used to induce BBB characteristics could be used to mimic
494 possible brain tissue binding. Finally, the calculation of P_{vitro} in presence and absence (i.e.
495 uncoupling with non-specific binding) of the brain cells in these assays might facilitate the
496 clarification of the influence of brain tissue binding on the distribution of different compounds
497 across the BBB.

498

499 5. Acknowledgements

500 The authors warmly thank Mila Renftel, for her assistance with this study and the European
501 Commission for its support under a Marie Skłodowska-Curie Innovative Training Network:
502 BtRAIN – European Brain Barriers Training Network (H2020-MSCA-ITN-2015, n°675619).

503

504 6. Table Legends

505 **Table 1** – *In vitro* BBB permeability values for the 27 CNS drugs under study obtained by the traditional
506 method (P_{app} and P_e). The permeability values are accompanied by their corresponding (average) mass
507 balance value (MB). The MB was also measured in absence of bovine brain capillary endothelial cells
508 (bBCEC or EC).

509

510 **Table 2** – Physico-chemical characteristics: fraction unbound brain ($f_{u,br}$) and lipophilicity (LogP) and the
511 *in vivo* blood-brain barrier (BBB) permeability (P_{vivo}) for the 27 CNS drugs under study determined by
512 Summerfield et al. (2007) [6].

513

514 **Table 3** – *In vitro* BBB permeability values obtained for the 27 CNS drugs under study by the new method
515 to assess BBB permeability (P_{vitro}). Permeability values are given for measurements in presence of glial
516 cells and consist of a corresponding (average) mass balance value (MB).

517

518 **Table 4** – In vitro BBB permeability values obtained for 3 CNS drugs (i.e. carbamazepine, diazepam and
519 chlorpromazine) by the new method to assess BBB permeability in vitro (P_{vitro}). The P_{vitro} values are given
520 for measurements in presence and absence of glial cells (GC) and consist of a corresponding (average)
521 mass balance value (MB). The MB for the condition without bBCEC (or EC) is also given.

522

523 **7. Figure Legends**

524 **Figure 1** – Relationship between in vivo brain permeability (P_{vivo}), obtained by brain perfusion in rodents,
525 taken from Summerfield et al. (2007) [6], and in vitro BBB permeability, either depicted by the apparent
526 permeability (P_{app}) (Graph A, C, E and G), or by the endothelial permeability (P_e) (Graph B, D, F and H),
527 and this for compounds of decreasing $f_{u,br}$.

528

529 **Figure 2** – Differences in $f_{u,br}$ depending on the experimental design of the model: A) In-situ rat BBB model,
530 B) In vitro bovine BBB model (consisting of bBCEC) without glial cells (GC) in the receiver compartment
531 during the drug permeability experiment; and C) In vitro BBB model (consisting of bBCEC) with GC in the
532 receiver compartment during the drug permeability experiment.

533

534 **Figure 3** – Relationship between $f_{u,br}$ and A) $P_{\text{vivo}}/P_{\text{app}}$; and B) P_{vivo}/P_e . Regression analysis included all
535 compounds ($n = 27$). P_{vivo} values used for the different ratios were taken from Summerfield et al. (2007)
536 [6].

537

538 **Figure 4** – A) General scheme of the in vitro BBB model from Dehouck et al. (1990) [15]. Bovine brain
539 capillary endothelial cells (bBCEC) are cultured on the upper side of a permeable support and primary rat
540 glial cells (astrocytes, oligodendrocytes and microglia) are cultured at the bottom of the well. B)
541 Relationship between in vivo brain permeability (P_{vivo}), taken from Summerfield et al. (2007) [6], obtained
542 by brain perfusion in rodents, and in vitro BBB permeability, obtained by the new in vitro method (P_{vitro})
543 for all 27 compounds under study.

544

545 **Figure 5** – Comparison of P_{vitro} in presence and absence of glial cells for 3 compounds (i.e. carbamazepine,
546 diazepam and chlorpromazine) characterized by a different $f_{u,br}$.

547

548 **8. References**

- 549 [1] D.E. Pankevich, B.M. Altevogt, J. Dunlop, F.H. Gage, S.E. Hyman, Improving and accelerating
550 drug development for nervous system disorders, *Neuron*. 84 (2014) 546–553.
551 doi:10.1016/j.neuron.2014.10.007.
- 552 [2] R. Cecchelli, V. Berezowski, S. Lundquist, M. Culot, M. Renftel, M.-P. Dehouck, L. Fenart,
553 Modelling of the blood-brain barrier in drug discovery and development, *Nat. Rev. Drug Discov.*
554 6 (2007) 650–661. doi:10.1038/nrd2368.
- 555 [3] H.C. Helms, N.J. Abbott, M. Burek, R. Cecchelli, P.-O. Couraud, M.A. Deli, C. Förster, H.J. Galla,
556 I.A. Romero, E. V Shusta, M.J. Stebbins, E. Vandenhoute, B. Weksler, B. Brodin, In vitro models
557 of the blood-brain barrier: An overview of commonly used brain endothelial cell culture models
558 and guidelines for their use, *J. Cereb. Blood Flow Metab.* 36 (2016) 862–890.
559 doi:10.1177/0271678X16630991.

- 560 [4] M. Hammarlund-udenaes, M. Fridén, S. Syvänen, A. Gupta, On the rate and extent of drug
561 delivery to the brain, *Pharm.Res.* 25 (2008) 1737–1750. doi:10.1007/s11095-007-9502-2.
- 562 [5] M. Spreafico, M.P. Jacobson, In silico prediction of brain exposure: drug free fraction, unbound
563 brain to plasma concentration ratio and equilibrium half-life, *Curr. Top. Med. Chem.* 13 (2013)
564 813–820. doi:10.1016/j.biotechadv.2011.08.021.Secreted.
- 565 [6] S.G. Summerfield, K. Read, D.J. Begley, T. Obradovic, I.J. Hidalgo, S. Coggon, A. V Lewis, R.A.
566 Porter, P. Jeffrey, G. Abington, U.K.S. C, Central nervous system drug disposition: The
567 relationship between in situ brain permeability and brain free fraction, *J. Pharmacol. Exp. Ther.*
568 322 (2007) 205–213. doi:10.1124/jpet.107.121525.
- 569 [7] X. Liu, B.J. Smith, C. Chen, E. Callegari, S.L. Becker, X. Chen, J. Cianfrogna, A.C. Doran, S.D.
570 Doran, J.P. Gibbs, N. Hosea, J. Liu, F.R. Nelson, M. a Szewc, J. Van Deusen, Use of a
571 physiologically based pharmacokinetic model to study the time to reach brain equilibrium: An
572 experimental analysis of the role of blood-brain barrier permeability, plasma protein binding,
573 and brain tissue binding, *J. Pharmacol. Exp. Ther.* 313 (2005) 1254–1262.
574 doi:10.1124/jpet.104.079319.for.
- 575 [8] J.C. Kalvass, T.S. Maurer, Influence of nonspecific brain and plasma binding on CNS exposure:
576 Implications for rational drug discovery, *Biopharm. Drug Dispos.* 23 (2002) 327–338.
577 doi:10.1002/bdd.325.
- 578 [9] M. Friden, A. Gupta, M. Antonsson, U. Bredberg, M. Hammarlund-Udenaes, In vitro methods
579 for estimating unbound drug concentrations in the brain interstitial and intracellular fluids,
580 *Drug Metab. Dispos.* 35 (2007) 1711–1719. doi:10.1124/dmd.107.015222.
- 581 [10] X. Liu, C. Chen, B.J. Smith, Progress in brain penetration evaluation in drug discovery and
582 development, *J. Pharmacol. Exp. Ther.* 325 (2008) 349–356.
583 doi:10.1124/jpet.107.130294.strict.
- 584 [11] S. Becker, Xingrong Liu, Evaluation of the utility of brain slice methods to study brain
585 penetration, *Drug Metab. Dispos.* 34 (2006) 855–861.
586 doi:10.1124/dmd.105.007914.concentration.
- 587 [12] S.G. Summerfield, A.J. Stevens, L. Cutler, C. Osuna, B. Hammond, S. Tang, A. Hersey, D.J.
588 Spalding, P. Jeffrey, Improving the in vitro prediction of in vivo central nervous system
589 penetration: Integrating permeability, P-glycoprotein efflux, and free fractions in blood and
590 brain, *J. Pharmacol. Exp. Ther.* 316 (2006) 1282–1290. doi:10.1124/jpet.105.092916.features.
- 591 [13] Q.R. Smith, Y. Takasato, Kinetics of amino acid transport at the blood-brain barrier studied
592 using an in situ brain perfusion technique, *Ann. N. Y. Acad. Sci.* 481 (1986) 186–201.
593 doi:10.1111/j.1749-6632.1986.tb27150.x.
- 594 [14] M. Culot, S. Lundquist, D. Vanuxeem, S. Nion, C. Landry, Y. Delplace, M.-P. Dehouck, V.
595 Berezowski, L. Fenart, R. Cecchelli, An in vitro blood-brain barrier model for high throughput
596 (HTS) toxicological screening, *Toxicol. Vitro.* 22 (2008) 799–811. doi:10.1016/j.tiv.2007.12.016.
- 597 [15] M. -P Dehouck, S. Méresse, P. Delorme, J. -C Fruchart, R. Cecchelli, An easier, reproducible, and
598 mass-production method to study the blood–brain barrier In vitro, *J. Neurochem.* 54 (1990)
599 1798–1801. doi:10.1111/j.1471-4159.1990.tb01236.x.
- 600 [16] M.B. Bornstein, Reconstituted rat tail collagen used as a substrate for time tissue cultures on
601 coverlips in Maximow slides and roller tubes, *Lab. Invest.* 7 (1958) 134–139.
- 602 [17] A. Siflinger-Birnboim, P.J. Del Vecchio, J.A. Cooper, F.A. Blumenstock, J.M. Shepard, A.B. Malik,
603 Molecular sieving characteristics of the cultured endothelial monolayer, *J. Cell. Physiol.* 132
604 (1987) 111–117. doi:10.1002/jcp.1041320115.
- 605 [18] S. Lundquist, M. Renftel, J. Brillault, L. Fenart, R. Cecchelli, M.P. Dehouck, Prediction of drug

- 606 transport through the blood-brain barrier in vivo: A comparison between two in vitro cell
607 models, *Pharm.Res.* 19 (2002) 976–981. pm:12180550.
- 608 [19] M.-P. Dehouck, S. Méresse, P. Delorme, J.-C. Fruchart, R. Cecchelli, An Easier, Reproducible,
609 and Mass-Production Method to Study the Blood–Brain Barrier In Vitro, *J. Neurochem.* 54
610 (1990) 1798–1801. doi:10.1111/j.1471-4159.1990.tb01236.x.
- 611 [20] R. Cecchelli, S. Aday, E. Sevin, C. Almeida, M. Culot, L. Dehouck, C. Coisne, B. Engelhardt, M.
612 Dehouck, L. Ferreira, A stable and reproducible human blood-brain barrier model derived from
613 hematopoietic stem cells, *PLoS One.* 9 (2014). doi:10.1371/journal.pone.0099733.
- 614 [21] E.S. Lippmann, A. Al-Ahmad, S.P. Palecek, E. V Shusta, Modeling the blood–brain barrier using
615 stem cell sources, *Fluids Barriers CNS.* 10 (2013). doi:10.1186/2045-8118-10-2.
- 616